Nitrogen Ligation to Manganese in the Photosynthetic Oxygen-Evolving Complex: Continuous-Wave and Pulsed EPR Studies of Photosystem II Particles Containing ^{14}N or ^{15}N†

Victoria J. DeRose,‡,§ Vittal K. Yachandra,§ Ann E. McDermott,‡,§,∥ R. David Britt,§,⊥ Kenneth Sauer,*,‡,§ and Melvin P. Klein*,§

Department of Chemistry and Chemical Biodynamics Division, Lawrence Berkeley Laboratory, University of California, Berkeley, California 94720

Received April 6, 1990; Revised Manuscript Received August 13, 1990

ABSTRACT: The possibility of nitrogen ligation to the Mn in the oxygen-evolving complex from photosystem II was investigated with electron paramagnetic resonance (EPR) and electron spin echo envelope modulation (ESEEM) spectroscopies using ^{14}N- and ^{15}N-labeled preparations. Oxygen-evolving preparations were isolated from a thermophilic cyanobacterium, *Synechococcus* sp., grown on a medium containing either $^{14}NO_3^-$ or $^{15}NO_3^-$ as the sole source of nitrogen. The substructure on the "multiline" EPR signal, which arises from Mn in the S_2 state of the enzyme, was measured with continuous-wave EPR. No changes were detected in the substructure peak positions upon substitution of ^{15}N for ^{14}N, indicating that this substructure is not due to superhyperfine coupling from nitrogen ligands. To detect potential nitrogen ligands with superhyperfine couplings of lesser magnitude than could be observed with conventional EPR methods, electron spin-echo envelope modulation experiments were also performed on the multiline EPR signal. The Fourier transform of the light-minus-dark time domain ESEEM data shows a peak at 4.8 MHz in ^{14}N samples which is absent upon substitution with ^{15}N. This gives unambiguous evidence for weak hyperfine coupling of nitrogen to the Mn of the oxygen-evolving complex. Possible origins of this nitrogen interaction are discussed.

The photosystem II oxygen-evolving complex (OEC) in green plants and cyanobacteria catalyzes the photon-driven oxidation of two molecules of H_2O to one molecule of O_2. The OEC is a membrane-bound complex consisting of several polypeptides and electron-transfer cofactors. The complex contains four Mn atoms which have been postulated to form the site(s) of water binding and oxidation. While EPR and X-ray absorption spectroscopies have provided information about the arrangement of the Mn [for review, see Babcock (1987), Pecoraro (1988), and Sauer et al. (1991)], the nature of the terminal ligands is not yet known. Ligands for the Mn have been proposed to come from amino acids in regions of the D_1 and D_2 polypeptides, near the carboxy termini, which are highly conserved among water-oxidizing species [reviewed in Babcock et al. (1989)]. These conserved sequences contain many carboxylic acid residues as well as several histidines, both of which are common ligands in metalloproteins.

The four-electron process of water oxidation in the OEC is coupled to the photooxidation of the pigment P_{680} through an intermediate tyrosine radical species (Barry & Babcock, 1987) and proceeds through five intermediates known as S states (Kok et al., 1970). X-ray absorption edge spectroscopy has been used to show that Mn undergoes a change in oxidation state as the S state of the complex is changed (Goodin et al., 1984; Guiles et al., 1990a,b; Yachandra et al., 1987). The results from extended X-ray absorption fine structure (EXAFS) studies indicate minimal units of oxo-bridged structures, where each Mn has one or two Mn neighbors at 2.7 Å and one or two bridging O ligand atoms at 1.8 Å (Yachandra et al., 1987; McDermott et al., 1988; Guiles et al., 1990a,b). A feature at ca. 3.3 Å which potentially results from another Mn-Mn interaction has also been detected (Yachandra et al., 1986b; George et al., 1988; Penner-Hahn et al., 1990). The EXAFS studies also indicate that each Mn has several O or N terminal ligand atoms at distances between 1.9 and 2.2 Å. The Mn-Mn distances and coordination numbers have allowed testing for the presence of structures resembling a variety of recently synthesized Mn complexes including dinuclear, trinuclear, and tetranuclear centers. Since EXAFS is not very sensitive to differences between first row elements, however, it is not possible to use it to discriminate between O or N in the terminal ligands.

The S_2 state of the OEC, which can be trapped with low-temperature illumination of dark-adapted preparations, is paramagnetic and gives rise to a multiline EPR signal centered at $g = 2$ (Dismukes & Siderer, 1981; Hansson & Andréasson, 1982). At X-band this EPR signal contains 16 or more Mn hyperfine lines, separated by approximately 80 G, which result from at least two exchange-coupled Mn nuclei. Each hyperfine line on the EPR multiline signal exhibits further substructure of three or four partially resolved peaks with 10-30-G separation (Yachandra et al., 1986a; Nugent, 1987; Hansson et al., 1986; Andréasson, 1989). Both additional Mn hyperfine transitions and superhyperfine coupling from ligands with

† This is paper 13 in the series "The State of Manganese in the Photosynthetic Apparatus". This research was supported, in part, by the Director, Office of Energy Research, Office of Basic Energy Sciences, Division of Energy Biosciences of the U.S. Department of Energy, under Contract DE-AC03-76SF00098, by a grant from the U.S. Department of Agriculture, (85-CRCR-1-1847), and by a grant from the National Science Foundation (DMB88-04526). A preliminary account of this work was presented at the VIIIth International Conference on Photosynthesis (Britt et al., 1990).

* Authors to whom correspondence should be addressed.

‡ Department of Chemistry.

§ Chemical Biodynamics Division, Lawrence Berkeley Laboratory.

∥ Present address: Department of Chemistry, Columbia University, New York, NY.

⊥ Present address: Department of Chemistry, University of California, Davis, CA.

0006-2960/91/0430-1335$02.50/0

paramagnetic nuclei have been proposed to contribute to the substructure of the multiline signal. The magnitude of the superhyperfine interaction may be very small, however, compared with the inhomogeneous width of the Mn hyperfine lines. Studies have attempted to gain evidence for superhyperfine interactions from exchangeable Cl^- ligands or from protons by measuring the multiline signal substructure in samples which have been washed with Br^- and ^2H_2O, respectively. In one study, after exchange with ^2H_2O a slight increase in resolution of the substructure features was reported (Nugent, 1987), but others have found no such effect (Yachandra et al., 1986a; Haddy et al., 1989). No detectable change in line width was reported after exchange of Cl^- with Br^- (Yachandra et al., 1986a; Haddy et al., 1989). A comparison between chloroplast preparations from spinach grown hydroponically in ^{15}N and ^{14}N also showed no detectable line width changes in the multiline signal (Andréasson, 1989). From this it was concluded that nitrogen hyperfine coupling to the manganese was very unlikely. Since the nitrogen hyperfine interaction may be very small, however, a negative result with this kind of experiment does not prove the absence of an interaction.

Electron spin-echo envelope modulation (ESEEM)[1] is a more sensitive method of measuring superhyperfine couplings in such systems with large inhomogeneous broadening (Mims & Peisach, 1981; Kosman, 1984). The amplitude of the spin echo induced by a pulse sequence is modulated through the interaction of the electron spin with nearby paramagnetic nuclei. The modulation frequencies can be directly related to the nuclear Zeeman and hyperfine interactions, as well as the electric quadrupole interactions for nuclei with spin $I \geq 1$. Recently, the weak hyperfine coupling of directly ligating nitrogen from the bipyridal ligands in the model compound di-μ-oxo-bridged dimanganese(III, IV) bipyridine complex has been measured by using ESEEM (Britt, 1988; Britt et al., 1991). This binuclear complex presents a 16-line EPR spectrum which is very similar to the multiline signal from the OEC. The ^{14}N isotropic hyperfine coupling of approximately 1 G determined by ESEEM is too small to be detected on the 40 G wide Mn hyperfine lines by using continuous-wave EPR (Britt et al., 1991). ESEEM has also been successful in demonstrating the binding of ammonia (an inhibitor and potential substrate analogue) to Mn in the OEC from spinach, again with an isotropic hyperfine coupling of approximately 1 G (Britt et al., 1989). No difference in line width of the multiline signal between $^{14}NH_3$- and $^{15}NH_3$-substituted samples was detected by CW EPR (Beck et al., 1986).

The ESEEM spectrum of the multiline signal from the native OEC of spinach contains modulation at two frequencies, ca. 14 and 5 MHz (Britt et al., 1989). The modulation at 14 MHz is assigned to weak interactions with nearby matrix protons (Britt, 1988). The 5-MHz peak has remained unassigned but could be due to interaction with a nearby ^{14}N nucleus. This is tested in the present study using PSII OEC preparations from the cyanobacteria *Synechococcus* sp. grown in media containing either $^{15}NO_3^-$ or $^{14}NO_3^-$ as the sole source of nitrogen. The EPR (Aasa et al., 1987; McDermott et al., 1988) and Mn X-ray absorption spectroscopic results (McDermott et al., 1988) to date indicate that the OEC from thermophilic cyanobacteria is remarkably similar to that from spinach. The effects of nitrogen isotope substitution on the ESEEM spectrum and the CW EPR spectrum of the multiline EPR signal from *Synechococcus* are reported.

[1] Abbreviations: ESEEM, electron spin-echo envelope modulation; Chl *a*, chlorophyll *a*; DCBQ, dichlorobenzoquinone; PMSF; phenylmethanesulfonyl fluoride; EDTA; ethylenediaminetetraacetic acid; MES, 4-morpholineethanesulfonic acid; DMSO, dimethyl sulfoxide.

Materials and Methods

Synechococcus sp. Growth and PSII OEC Isolation. Ten-liter cultures of *Synechococcus* sp. were grown at 50–55 °C. The growth medium was modified from that in McDermott et al. (1988) such that all added nitrogen was in the form of KNO_3. EDTA was excluded from the medium. As PSII preparations from cyanobacteria grown in medium containing 50 μM Cu^{2+} had a broad background EPR signal at $g = 2.2$, Cu^{2+} was also excluded from the growth medium for these experiments. It was found that the total nitrogen concentration could be decreased from 11 mM in the original medium to 4 mM, which slowed the growth rates but did not adversely affect the final yield of active PSII. Enrichment with ^{15}N was performed by growing the bacteria in medium containing $K^{15}NO_3$ (99%, MSD Isotopes) through two inoculations, such that the volume of original ^{14}N inoculant in the final ^{15}N growth medium was 0.05%.

Oxygen evolution activity was measured at 24 °C with a Clark-type electrode illuminated with a slide projector lamp (McDermott et al., 1988). The measurement buffer was 50 mM MES pH 6.0, 5 mM $CaCl_2$, 400 mM sucrose, 200 μM PMSF, and 2 mM DCBQ (diluted from a stock solution of 200 mM DCBQ dissolved in DMSO).

Oxygen-evolving PSII complexes from *Synechococcus* were isolated from thylakoids having specific O_2 activities of 300–500 μmol of O_2 (mg of Chl·h)$^{-1}$ according to the method described by McDermott et al. (1988). The PSII preparations typically exhibited activities of 2500–4000 μmol of O_2 (mg of Chl·h)$^{-1}$ with 60–75 Chl per PSII. Detergent-extracted PSII complexes were pelleted by centrifugation at 4 °C, 300000*g*, for 3–4 h. The pellet was resuspended in sucrose buffer (50 mM Mes, pH 6.5, 5 mM $CaCl_2$, 400 mM sucrose, pH 6.5, 200 μM PMSF) and centrifuged as before, then resuspended in the same buffer minus sucrose and containing 1 mM EDTA, and centrifuged as above for 2 h. The pellet was then resuspended in a mixture of 50% buffer (with EDTA)/50% glycerol to 2–3 mg of Chl/mL. Samples were loaded into EPR tubes and dark-adapted on ice for at least 30 min before being stored at 77 K. For illumination at 200 K, samples were immersed in a methanol/solid CO_2 bath and illuminated for 5–10 min with a 400-W tungsten lamp thermally isolated from the sample by a 5-cm water filter containing 5% aqueous $CuSO_4$.

^{15}N Enrichment Determination. ^{15}N content was determined from the mass spectrum of Chl *a* by using an AEI MS12 low-resolution mass spectrometer following ionization at 10 eV. Comparison of the ratios of the parent and M-1 peaks of Chl *a* from ^{14}N- and ^{15}N-grown bacteria showed >95% labeling with ^{15}N. Chl *a* was isolated from *Synechococcus* by using a preparation slightly modified from that of Omata and Murata (1983).

Electron Paramagnetic Resonance. EPR at X-band was performed by using a Varian E-109 spectrometer with a standard TE_{102} cavity. A GaAsFET amplifier (Dexheimer & Klein, 1988) was used for spectra taken at 5-mW power. Individual scans were collected by using a signal averager of local design interfaced with a VAX 11/785 computer. The sample temperature was maintained at 8.0 ± 0.5 K with an Air Products liquid helium cryostat.

Electron Spin-Echo Spectroscopy. Two-pulse ESE spectroscopy was performed at 4.2 K by using a home-built spectrometer with a cryogenic loop-gap resonator probe (Britt & Klein, 1987; Britt et al., 1989). Microwave pulses, 200 W, were of 12-ns duration. The instrument dead time was 120

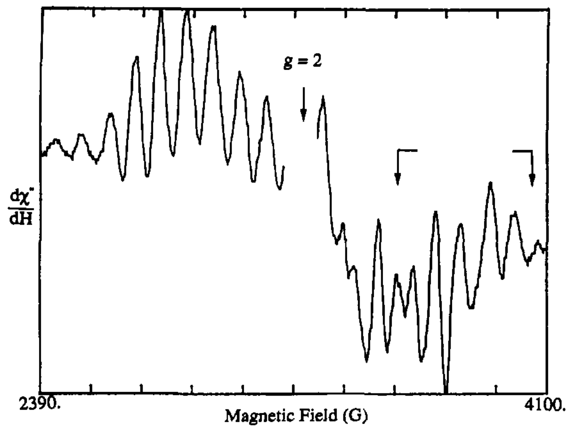

FIGURE 1: Continuous-wave EPR spectrum of PSII OEC preparations from *Synechococcus* sp. (grown on ^{14}N) in the S_2 state. The spectrum was recorded after advancement to the S_2 state following a 4-min illumination at 200 K of a dark-adapted sample, and the spectrum of the dark-adapted sample is subtracted. A narrow region of the spectrum at $g = 2$ is removed due to a sharp feature from the subtraction. Spectra were recorded at 9.2 GHz, 30-mW power, 8 K, 25-G modulation amplitude, 5000 gain, and 100-kHz modulation frequency. Chlorophyll concentration is 2–3 mg/mL. Arrows indicate boundaries of the region which is examined in detail in Figure 2.

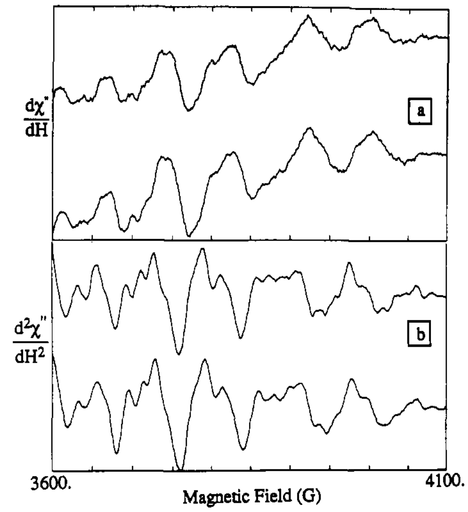

FIGURE 2: (a) Continuous-wave EPR spectra comparing the multiline substructure in PSII OEC preparations from *Synechococcus* sp. grown on ^{14}N (upper trace) and ^{15}N (lower trace). Spectra are averages of 50 scans, 2 min each, recorded at 9.2 GHz, 5 mW, 4-G modulation amplitude, 100-kHz modulation frequency, 8.0 ± 0.5 K, and 1×10^5 gain. Samples were illuminated at 200 K for 4 min. (b) Comparison of the first derivatives of the data shown in (a) (second derivatives of the absorption). The upper trace is from *Synechococcus* grown on ^{14}N and the lower trace from *Synechococcus* grown on ^{15}N. The derivatives were calculated from a second-order polynomial fit to a sliding window of 16 G. A comparison of individual peak positions shows them to be indistinguishable within ± 2 G.

ns. The two-pulse time domain data were acquired by gated integration of the spin-echo signal as a function of interpulse time τ, which was increased in 10-ns increments. The cosine Fourier transforms are presented with short experimental dead times reconstructed by using the Fourier backfill technique described by Mims (1984).

Results

Continuous-Wave EPR of the Multiline Signal from ^{14}N- and ^{15}N-Grown Synechococcus. Figure 1 shows an EPR spectrum of a 200 K illuminated PSII sample from ^{14}N-grown *Synechococcus*, after subtraction of the spectrum of the dark-adapted sample. As previously reported (Aasa et al., 1987; McDermott et al., 1988), the multiline signal is very similar to that from spinach in terms of the number and splittings of the hyperfine lines. A slight difference in line shape from *Synechococcus* on the high-field side of $g = 2$ can be ascribed to a small amount of an underlying signal at $g = 1.6$, which has been assigned as a reduced acceptor species (McDermott et al., 1988). That signal contributes to the spectrum as a broad, featureless absorption from 3700 to 4000 G.

Figure 2 shows signal-averaged spectra of the high-field side of the multiline signal recorded at 4-G modulation amplitude and 5-mW power. Under these conditions, the individual lines can be seen to have asymmetric shapes, which are split or have shoulders with 10–30-G separation. Figure 2a is from cyanobacterial preparations grown on $^{14}NO_3^-$ (upper trace) and $^{15}NO_3^-$ (lower trace). There are no obvious differences between the two preparations in the shapes or splittings of the Mn hyperfine lines. The second derivatives of the absorption line, calculated from the first derivative of a sliding polynomial fit to the spectra, are compared in Figure 2b. These second derivative spectra show no systematic changes in peak positions, indicating that at 4-G spectrometer resolution no change in line shape is evident in the multiline EPR signal due to the substitution of ^{15}N for ^{14}N in the cyanobacterial OEC.

ESEEM of ^{15}N- and ^{14}N-Grown Synechococcus PSII. Figure 3 displays the ESEEM patterns following a two-pulse sequence at a field of 3200 G on the multiline signal from a ^{14}N-grown *Synechococcus* sp. PSII sample. Both the time domain data (Figure 3a) and the cosine Fourier transform (Figure 3b) are shown. Peaks are observed in the Fourier transform at 4.5 and 13.6 MHz. Comparable features were observed in ESEEM spectra obtained at 3100 and 3400 G (data not shown). These features are very similar to those observed in PSII preparations from spinach (Britt et al., 1989). The 13.6-MHz peak arises from weak coupling to protons, some of which in spinach are exchanged upon short (4-h) incubation in ^2H_2O-enriched buffer (Britt et al., 1990).

Panels a and b of Figure 4 show the ESEEM time domain data and Fourier transform of the multiline signal from a ^{15}N *Synechococcus* PSII preparation, respectively. The modulation at around 4.5 MHz is absent in these data, which were taken at 3200 G, as well as in data taken at 3100 and 3400 G (data not shown). The absence of the 4.5-MHz peak in the ^{15}N data indicates that the feature arises from coupling of the electron spin to one or more ^{14}N in the vicinity of the manganese cluster. No corresponding feature due to ^{15}N appears in the data taken at 3200 G (Figure 4b) or 3100 or 3400 G (data not shown).

Nitrogen Modulation in Dark-Adapted Samples. A comparison of the Fourier transforms of ESEEM at 3200 G of the dark-adapted ^{14}N and ^{15}N samples is shown in panels a and b of Figure 5. The ^{15}N sample shows modulation at $\sim$1.3 and $\sim$4.8 MHz, whereas the ^{14}N sample has modulation at $\sim$4 and $\sim$7 MHz. This modulation is most likely due to nitrogen ligation to Fe^{3+} in oxidized cytochrome b_{559}. The continuous-wave EPR spectra of these dark-adapted PSII preparations show large signals at $g = 3.0$ and 2.2 which arise from the oxidized cytochrome, as well as a signal at $g = 6$ which resembles oxidized high-spin ferricytochrome (data not shown). In its reduced form, cytochrome b_{559} is an alternative electron donor to P_{680}^+ at temperatures below 200 K (dePaula et al., 1985). For the ESEEM experiments on the multiline signal from *Synechococcus*, the amplitude of the signals at $g = 3.0$ and $g = 6.0$ were monitored with CW EPR before and after the 200 K illumination to show that no additional oxidized cytochrome b_{599} was formed during the illumination.

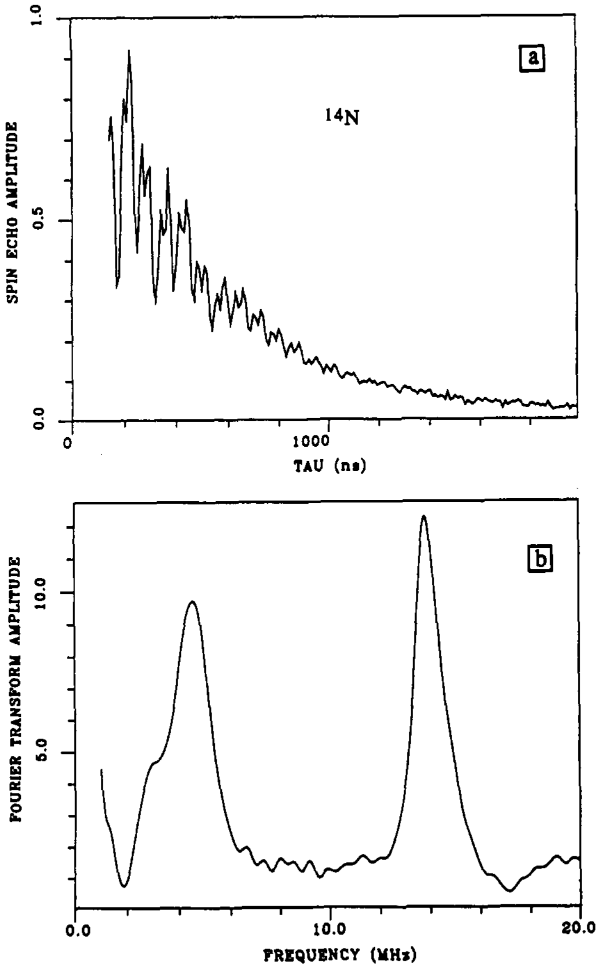

FIGURE 3: Amplitude of the spin echo, as a function of τ after a two-pulse sequence, from the multiline signal from PSII OEC preparations from *Synechococcus* sp. grown on $^{14}NO_3^-$ (a). The subtracted data (200 K illuminated samples minus dark-adapted samples) are shown. The cosine Fourier transform shows peak at ca. 14 and 4.5 MHz in the ^{14}N spectrum (b). The peak at around 14 MHz is due to protons and is centered at the proton Larmor frequency. Spectrometer conditions were 9.2-GHz microwave frequency, 4.2 K, and 3200-G field position. The spectra are the average of 15 scans. The intervals τ between pulses in the two-pulse sequence were increased by 10-ns increments, with a 2.5-ms interval between each two-pulse sequence.

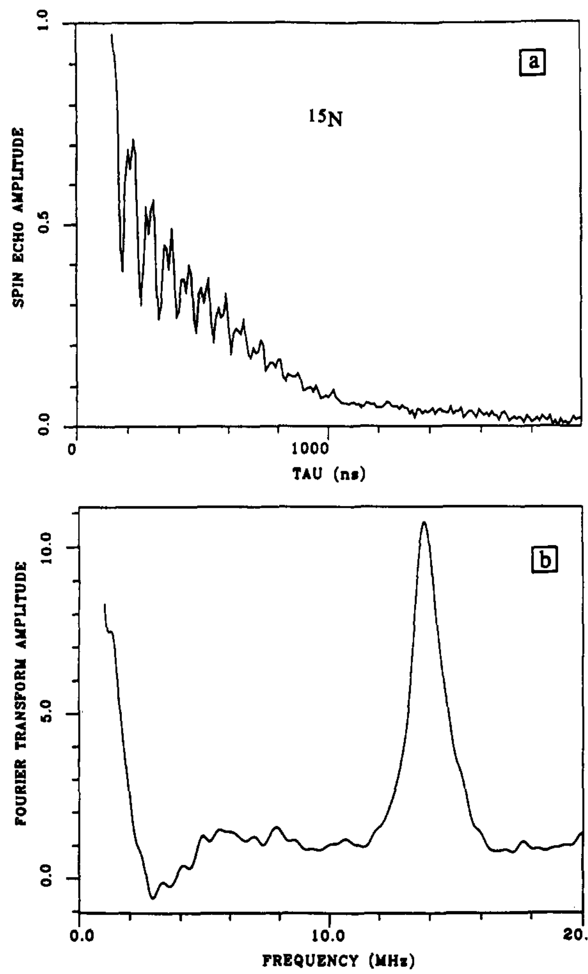

FIGURE 4: Amplitude of the spin echo (a) and the cosine Fourier transform (b) from the multiline signal from PSII OEC preparations from *Synechococcus* sp. grown on $^{15}NO_3^-$. In contrast to the spectra for the ^{14}N-enriched samples (Figure 3), the ^{15}N Fourier transform shows only the peak centered at the proton Larmor frequency of ~14 MHz. Spectrometer conditions were as in Figure 3.

Thus, the frequencies in the light-minus-dark ESEEM data are due only to the multiline species.

Discussion

In this study, the question of nitrogen ligation to the Mn in the PSII oxygen-evolving complex was addressed by using both pulsed and continuous-wave EPR on ^{15}N-substituted samples from the thermophilic cyanobacterium *Synechococcus* sp. The ESEEM of the multiline signal from the *Synechococcus* OEC was found to have the same frequency components as the OEC from spinach. The ESEEM frequency at ~4.5 MHz disappeared upon total isotopic substitution with ^{15}N, giving unambiguous evidence for weak hyperfine interaction of nitrogen with the Mn of the OEC.

In the dimanganese(III,IV) di-μ-oxo-bridged bipyridine compound, the magnitude of the isotropic hyperfine coupling of the *directly ligating* N has been determined by ESEEM to be less than 1 G (Britt, 1988; Britt et al., 1991). By contrast, in Cu–histidine or Cu–imidazole complexes the coupling between Cu and the ligating imino N of >30 MHz (>10 G) is greater than can be observed with conventional ESEEM (Mims & Peisach, 1978). We expect the hyperfine interactions to ligands in the OEC to resemble those in the dimanganese(III,IV) model compound, whose EPR spectrum is very similar to the OEC multiline EPR signal. However, we have also used continuous-wave EPR to show that in the OEC strong hyperfine interactions with nitrogen could not be detected by comparing the substructure on the multiline EPR signals from ^{14}N- and ^{15}N-substituted PSII samples.

What is the origin of the weak ^{14}N hyperfine interaction in the OEC? In some cases, the ESEEM frequencies of both ^{14}N- and ^{15}N-substituted samples allow an analysis of the nitrogen hyperfine and quadrupole coupling parameters [see, for example, Mims and Peisach (1978) and McCracken et al. (1988)]. These parameters can be used to describe the interacting species. Unfortunately, in this experiment modulation due to ^{15}N was not detected over the magnetic field range of the multiline signal at 9 GHz. Additionally, only one frequency due to ^{14}N is detected in both two-pulse and three-pulse (stimulated echo) experiments (Britt et al., 1991). It may therefore be necessary to extend the ESEEM measurements to microwave frequencies beyond the range of our X-band spectrometer to gain information about the specific parameters of nitrogen hyperfine coupling in the OEC. For both ^{15}N and ^{14}N nuclei, the ESEEM amplitudes will be maximal at a field position where the nuclear Zeeman frequency is half the magnitude of the hyperfine coupling constant

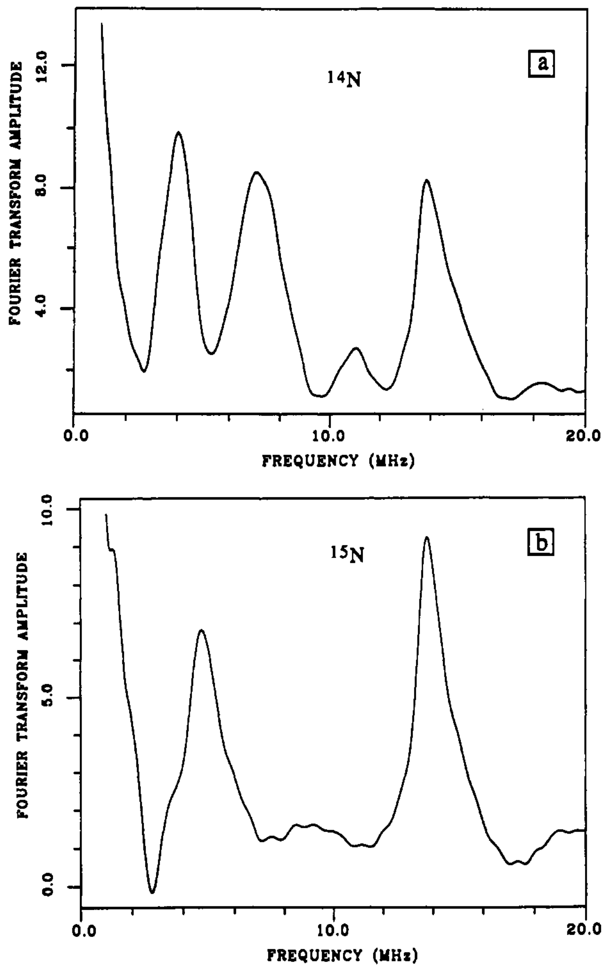

FIGURE 5: Comparison of the Fourier transform spectra of dark-adapted PSII OEC preparations from ^{14}N- and ^{15}N-grown *Synechococcus* sp. The cosine Fourier transforms of the time domain ESEEM pattern are shown. Peaks at ca. 4 and 7 MHz are found for the ^{14}N sample (a) and 1.2 and 4.8 MHz for the ^{15}N sample (b). Experimental conditions were as in Figure 4.

(Astashkin et al., 1984; DeGroot et al., 1986; Flanagan & Singel, 1987; Lai et al., 1988). For the $I = {}^1/_2$ ^{15}N nucleus, the field range over which the significant modulation is observed is determined by the magnitude of the anisotropic component of the hyperfine interactions (Lai et al., 1988), whereas the electric quadrupole interaction of the $I = 1$ ^{14}N nucleus enhances the modulation amplitude and increases the field range over which modulation from ^{14}N may be observed (Flanagan & Singel, 1987).

The high value of the ^{14}N ESEEM frequency (4.5 MHz at 3200 G) indicates that it is due to interactions with specific nitrogen nuclei in the immediate vicinity of the OEC Mn. It is unlikely that ^{14}N nuclei in a protein environment would have transitions at a frequency as high as 4.5 MHz without magnetic contributions from hyperfine contact interactions. Such a contact interaction could result either from ligation of a nitrogen directly to the Mn cluster or possibly from hydrogen bonding to a bridging oxygen of the Mn complex. Without such a contact interaction, the only magnetic contributions would be from the 3200-G applied field and a weaker dipolar field arising from the electronic spin. We estimate by numerical simulations [performed as described in Britt et al. (1989)] that, in the absence of a contact interaction, the value of the electric quadrupolar coupling parameter e^2qQ would have to exceed 4.0 MHz in order to generate a transition of 4.5 MHz. A quadrupolar coupling value of greater than 4.0 MHz is larger than expected for peptide nitrogens (e^2qQ between 3.0 and 3.4 MHz), amide nitrogens (e^2qQ approximately 2.5 MHz), or nitrogens in the imidazole side chain of histidine (e^2qQ of 3.4 MHz for the imino nitrogen, 1.4 MHz for the amino nitrogen) (Edmonds, 1976). We therefore consider it unlikely that the ^{14}N ESEEM transition observed at 4.5 MHz arises from one or more distant nitrogens.

A more likely source of the nitrogen interaction detected by ESEEM is through superhyperfine coupling between a nitrogen ligand from an amino acid and the unpaired spin on the manganese. The multiline EPR signal from the OEC shows very shallow nitrogen modulation in comparison with the model compound di-μ-oxo-bridged dimanganese(III, IV) bipyridine complex (Britt, 1988; Britt et al., 1991). This qualitative comparison would indicate few, perhaps one or two, nitrogen ligands in the OEC. It is important here to note that the nitrogen interaction detected in this study applies only to the manganese in the OEC which contribute to the multiline EPR signal, which may have a dominant contribution from only two or three of the four Mn in the complex. The proposed Mn-binding regions on the C-termini of the D_1 and D_2 polypeptides (Michel & Deisenhofer, 1988; Babcock et al., 1989), contain a lysine (K_{318} on D_2) and several histidine (H_{337} and H_{332} on D_1 and H_{337} on D_2) and arginine (R_{334}, R_{323}, and R_{312} on D_1 and R_{349}, R_{327}, and R_{305} on D_2) residues which are conserved among both cyanobacteria and higher plants (Gingrich et al., 1988, 1990). Additional conserved nitrogen-containing residues are found in regions which are predicted to be on the lumenal side of the membrane (Michel & Deisenhofer, 1988) between α-helices A and B (H_{92} and R_{64} on D_1, H_{62} and R_{104} on D_2) and C and D (H_{191} on D_1, H_{190} and R_{181} on D_2) (Gingrich et al., 1990). It is not possible to distinguish among these possibilities from the results of this experiment (vide supra). In all known structures of manganese-containing proteins, however, there is no nitrogen coordination other than that arising from histidine (Brookhaven Protein Data Bank). In recent work Guiles et al. (1990b) proposed a redox-active ligand in the OEC which becomes oxidized in the S_2 to S_3 state transition and suggested an aromatic amino acid such as a histidine for the identity of this ligand. Supporting this is the discovery of a broad, featureless EPR signal centered at $g = 2$, reported to arise from the S_3 state in samples that have been depleted of Ca^{2+} (Sivaraja et al., 1989; Boussac et al., 1989). This signal has tentatively been assigned to a histidine radical (Boussac et al., 1990). The involvement of histidine in binding Mn is also supported by chemical modification experiments, in which the use of a histidine-specific modifying agent was reported to inhibit the photoactivation of Mn-depleted PSII particles (Tamura et al., 1989).

An alternative possibility for the interaction of nitrogen with the Mn complex is through a hydrogen bond between an amino acid side chain or peptide amide and a Mn–Mn μ-oxo bridge or oxo ligand. Hydrogen bonding to metal bridging ligands is seen, for example, in Fe-S centers (Mino et al., 1987) and oxyhemerythrin (Shiemke et al., 1986). While it is not possible to rule out this type of interaction in the OEC, isotope exchange experiments using ^2H_2O may provide some information. The isotropic hyperfine coupling through a hydrogen bond would be expected to change significantly upon exchange in ^2H_2O, as ^2H in general forms weaker hydrogen bonds. The ^{14}N ESEEM peak in the OEC remains unchanged upon a 4-h exchange in ^2H_2O-enriched buffer, although approximately half of the protons contributing to the 15-MHz modulation component are replaced by deuterons (Britt, 1988; Britt et al., 1990). Because acidic protons are expected to exchange readily, this would indicate that the nitrogen modulation does not arise from an amide or amino group which is hydrogen-bonded to the Mn complex. For this test to be conclusive, however, it may be necessary to have prolonged exposure to ^2H_2O for complete exchange, especially if the site is buried in the interior of the protein.

To address the possibility of nitrogen hyperfine interactions in the OEC which are larger than could be observed by ESEEM, we have compared the continuous-wave EPR spectra of the ^{15}N- and ^{14}N-substituted PSII samples. It has been suggested that the substructure on the multiline EPR signal is due to partially resolved superhyperfine interactions from nitrogen ligands. Substitution of ^{15}N for ^{14}N produced no detectable change in the positions of the substructure features on the multiline EPR signal. For the simple case of resolved splitting due to an isotropic hyperfine interaction from a single N nucleus, substitution of ^{15}N ($I = {}^1/_2$) for ^{14}N ($I = 1$), where the nuclear moment ratio $g_n(^{15}N)/g_n(^{14}N)$ is 1.4, would collapse three peaks into two with the separation between the outermost peaks reduced by approximately 17%. With a modulation amplitude of 4 G, the narrowest features on the multiline signal that we could reliably resolve were positive peaks (in the first derivative) separated by approximately 10 G. Lowering the modulation amplitude to 2 G resolved no new features in the spectrum (data not shown). We thus estimate that the inability to detect consistent changes on the substructure of the multiline EPR signal upon substitution of ^{14}N with ^{15}N indicates the absence of nitrogen hyperfine coupling of magnitude $\geq$10 G. The substructure is most likely due to partially resolved Mn hyperfine interactions, as has been suggested from the results of previous experiments with spinach chloroplasts (Andréasson, 1989), experiments at S-band (Haddy et al., 1989), and ESEEM studies (Britt et al., 1989).

The dark-adapted samples of PSII from ^{14}N-grown *Synechococcus* show ESEEM at frequencies of 4 and 7 MHz. The predominant features in the continuous-wave EPR spectrum of these dark-adapted samples are signals at $g = 3.0$ and $g = 2.2$ from oxidized cytochrome b_{559}. The ^{14}N ESEEM is very similar to that reported for porphyrin ^{14}N in low-spin Fe^{3+} complexes (Peisach et al., 1979) and is consistent with an assignment as hyperfine interactions from the porphyrin nitrogens in oxidized cytochrome b_{559}. The Fourier transform of the ESEEM in dark-adapted PSII samples from ^{15}N-grown *Synechococcus* is shown in Figure 4b. Modulation occurs at 1.3 MHz, which is the ^{15}N Zeeman frequency at 3200 G. A shoulder is present on this Fourier transform peak at ~2 MHz, and the higher frequency modulation is at 4.8 MHz. Since ESEEM occurs at frequencies $|\nu_I \pm A/2|$ for $I = {}^1/_2$ species, the frequencies in the dark-adapted samples from ^{15}N-grown *Synechococcus* are consistent with their arising from a species with A_{iso} (for ^{15}N) of 7 MHz. This scales (by the ratio of the $^{14}N/^{15}N$ magnetic moments) to A_{iso} of 5 MHz for ^{14}N. This ^{15}N ESEEM could be due to hyperfine interactions from the porphyrin nitrogens, which were found to have an A_{iso} of 5 MHz for ^{14}N (Peisach et al., 1979). Alternatively, the ^{15}N ESEEM may arise from the postulated bis-imidazole coordination in cytochrome b_{559} (Babcock et al., 1985). ENDOR experiments on bis-imidazole Fe^{3+} porphyrin model complexes have determined a hyperfine coupling of 5 MHz for the directly coordinating ^{14}N of the imidazoles (Scholes et al., 1986). We note, however, that the continuous-wave EPR spectra of dark-adapted samples from *Synechococcus* also show a signal at $g = 6$, which potentially arises from high-spin Fe^{3+} from damaged cytochrome b_{559} (Rutherford, 1985). Since this signal may have counterparts in the $g = 2$ region, it is not possible to rule out contributions from damaged cytochrome to the ESEEM of the dark-adapted samples.

In conclusion, the results reported for ESEEM and CW EPR experiments on the multiline signal which arises from Mn in the S_2 state of the OEC indicate the presence of weak hyperfine coupling from one or more nearby ^{14}N. The ESEEM due to ^{14}N may be from an amino acid ligand, such as a histidine. It is not possible at this time to rule out an interaction with nitrogen which is hydrogen-bonded to the Mn complex. The identity of the interacting species is currently being sought through the development of auxotrophs for the putative amino acid ligands.

Acknowledgments

We express gratitude to A. Boussac, J.-L. Zimmermann, A. W. Rutherford, and J. Lavergne for communicating results prior to publication. The mass spectrum analyses of ^{14}N- and ^{15}N-labeled Chl were performed by the University of California—Berkeley Mass Spectrometry Laboratory.

Registry No. Mn, 7439-96-5; N_2, 7727-37-9.

References

Aasa, R., Andréasson, L.-E., Lagenfelt, G., & Vänngård, T. (1987) *FEBS Lett. 221*, 245–248.

Andréasson, L.-E. (1989) *Biochim. Biophys. Acta 973*, 465–467.

Astashkin, A. V., Dikanov, S. A., & Tsvetkov, Y. D. (1984) *J. Struct. Chem. 25*, 45–55.

Babcock, G. T. (1987) in *New Comprehensive Biochemistry: Photosynthesis 15* (Amesz, J., Ed.) pp 125–158, Elsevier, Amsterdam.

Babcock, G. T., Widger, W. R., Cramer, W. A., Oertling, W. A., & Metz, J. G. (1985) *Biochemistry 24*, 3638–3645.

Babcock, G. T., Barry, B. A., Debus, R. J., Hoganson, C. W., Atamian, M., McIntosh, L., Sithole, I., & Yocum, C. F. (1989) *Biochemistry 28*, 9557–9565.

Barry, B. A., & Babcock, G. (1987) *Proc. Natl. Acad. Sci. U.S.A. 84*, 7099–7103.

Beck, W. F., de Paula, J. C., & Brudvig, G. W. (1986) *J. Am. Chem. Soc. 108*, 4018–4022.

Boussac, A., Zimmermann, J.-L., & Rutherford, A. W. (1989) *Biochemistry 28*, 8984–8989.

Boussac, A., Zimmermann, J.-L., Rutherford, A. W., & Lavergne, J. (1990) *Nature 347*, 303–306.

Britt, R. D. (1988) Ph.D. Thesis, University of California—Berkeley, Lawrence Berkeley Laboratory Report LBL-25042.

Britt, R. D., & Klein, M. P. (1987) *J. Magn. Reson. 74*, 535–540.

Britt, R. D., Zimmermann, J.-L., Sauer, K., & Klein, M. P. (1989) *J. Am. Chem. Soc. 111*, 3522–3532.

Britt, R. D., DeRose, V. J., Yachandra, V. K., Kim, D. H., Sauer, K., & Klein, M. P. (1990) in *Current Research in Photosynthesis* (Baltscheffsky, M., Ed.) I.3.769, Kluwer Academic Publishers, The Netherlands.

Britt, R. D., DeRose, V. J., Chan, M. K., Armstrong, W. H., Sauer, K., & Klein, M. P. (1991) (submitted for publication).

DeGroot, A., Evelo, R., & Hoff, A. J. (1986) *J. Magn. Reson. 66*, 331–343.

dePaula, J. C., Innes, J. B., & Brudvig, G. W. (1985) *Biochemistry 24*, 8114–8120.

Dexheimer, S. L., & Klein, M. P. (1988) *Rev. Sci. Instrum. 59*, 764–766.

Dismukes, G. C., & Siderer, Y. (1981) *Proc. Natl. Acad. Sci. U.S.A. 78*, 274–278.

Edmonds, D. T. (1976) *Phys. Rep. 29*, 233–290.

Flanagan, H. L., & Singel, D. J. (1987) *J. Chem. Phys. 87*, 5606–5616.

George, G. N., Prince, R. C., & Cramer, S. P. (1988) *Science 243*, 789–791.

Gingrich, J. C., Buzby, J. S., Stirewalt, V. L., & Bryant, D. A. (1988) *Photosynth. Res. 16*, 83–99.

Gingrich, J. C., Gasparich, G. E., Sauer, K., & Bryant, D. A. (1990) *Photosynth. Res. 24*, 137–150.

Goodin, D. B., Yachandra, V. K., Britt, R. D., Sauer, K., & Klein, M. P. (1984) *Biochim. Biophys. Acta 767*, 209–216.

Guiles, R. D., Yachandra, V. K., McDermott, A. E., Cole, J. L., Dexheimer, S. L., Britt, R. D., Sauer, K., & Klein, M. P. (1990a) *Biochemistry 29*, 486–495.

Guiles, R. D., Zimmermann, J.-L., McDermott, A. E., Yachandra, V. K., Cole, J. L., Dexheimer, S. L., Britt, R. D., Wieghardt, K., Bossek, U., Sauer, K., & Klein, M. P. (1990b) *Biochemistry 29*, 471–485.

Haddy, A., Aasa, R., & Andrêasson, L.-E. (1989) *Biochemistry 28*, 6954–6959.

Hansson, Ö., & Andrêasson, L.-E. (1982) *Biochim. Biophys. Acta 679*, 261–268.

Hansson, Ö., Andrêasson, L.-E., & Vänngård, T. (1986) *FEBS Lett. 195*, 151–154.

Kok, B., Forbush, B., & McGloin, M. (1970) *Photochem. Photobiol. 11*, 457–476.

Kosman, D. J. (1984) in *Structural and Resonance Techniques in Biological Research* (Rousseau, D. L., Ed.) pp 183–222, Academic Press, Orlando.

Lai, A., Flanagan, H. L., & Singel, D. J. (1988) *J. Chem. Phys. 12*, 7161–7166.

McCracken, J., Pember, S., Benkovic, S. J., Villafranca, J. J., Miller, R. J., & Peisach, J. (1988) *J. Am. Chem. Soc. 110*, 1069–1074.

McDermott, A. E., Yachandra, V. K., Guiles, R. D., Cole, J. L., Dexheimer, S. L., Britt, R. D., Sauer, K., & Klein, M. P. (1988) *Biochemistry 27*, 4021–4031.

Michel, H., & Deisenhofer, J. (1988) *Biochemistry 27*, 1–7.

Mims, W. B. (1984) *J. Magn. Reson. 59*, 291–306.

Mims, W. B., & Peisach, J. (1978) *J. Chem. Phys. 69*, 4921–4930.

Mims, W. B., & Peisach, J. (1981) in *Biological Magnetic Resonance 3* (Berliner, L. J., & Reuben, J., Eds) pp 213–263, Plenum Press, New York.

Mino, Y., Loehr, T. M., Wada, K., Matsubara, H., & Sanders-Loehr, J. (1987) *Biochemistry 26*, 8059–8065.

Nugent, J. H. A. (1987) *Biochim. Biophys. Acta 893*, 184–189.

Omata, T., & Murata, N. (1983) *Plant Cell Physiol. 24*, 1093–1100.

Pecoraro, V. L. (1988) *Photochem. Photobiol. 48*, 249–264.

Peisach, J., Mims, W. B., & Davis, J. L. (1979) *J. Biol. Chem. 254*, 12379–12389.

Penner-Hahn, J. E., Fronko, R. M., Pecoraro, V. L., Yocum, C. F., Betts, S. D., & Bowlby, N. R. (1990) *J. Am. Chem. Soc. 112*, 2549–2557.

Rutherford, A. W. (1985) *Biochim. Biophys. Acta 807*, 189–201.

Sauer, K., Yachandra, V. K., Britt, R. D., & Klein, M. P. (1991) in *Manganese Redox Enzymes* (Pecoraro, V. L., Ed.) VCH Publishers, New York (in press).

Scholes, C. P., Falkowski, K. M., Chen, S., & Bank, J. (1986) *J. Am. Chem. Soc. 108*, 1660–1671.

Shiemke, A. K., Loehr, T. M., & Sanders-Loehr, J. (1986) *J. Am. Chem. Soc. 108*, 2437–2443.

Sivaraja, M., Tso, J., & Dismukes, G. C. (1989) *Biochemistry 28*, 9459–9464.

Tamura, N., Ikeuchi, M., & Inoue, Y. (1989) *Biochim. Biophys. Acta 973*, 281–289.

Yachandra, V. K., Guiles, R. D., Sauer, K., & Klein, M. P. (1986a) *Biochim. Biophys. Acta 850*, 333–342.

Yachandra, V. K., Guiles, R. D., McDermott, A. E., Britt, R. D., Cole, J., Dexheimer, S. L., Sauer, K., & Klein, M. P. (1986b) in *Journal de Physique 2* (Lagarde, P., Raoux, D., & Petiau, J., Eds.) pp C8-1121–1128, Editions de Physique, Les Ulis, France.

Yachandra, V. K., Guiles, R. D., McDermott, A. E., Cole, J. L., Britt, R. D., Dexheimer, S. L., Sauer, K. & Klein, M. P. (1987) *Biochemistry 26*, 5974–5981.